



**Politecnico
di Torino**

Department
of Structural, Geotechnical
and Building Engineering

EGU General
Assembly 2023

Towards a general constitutive model for snow

Gianmarco Vallero, Monica Barbero, Fabrizio Barpi,
Mauro Borri-Brunetto, Valerio De Biagi

Vienna, April 24th, 2023

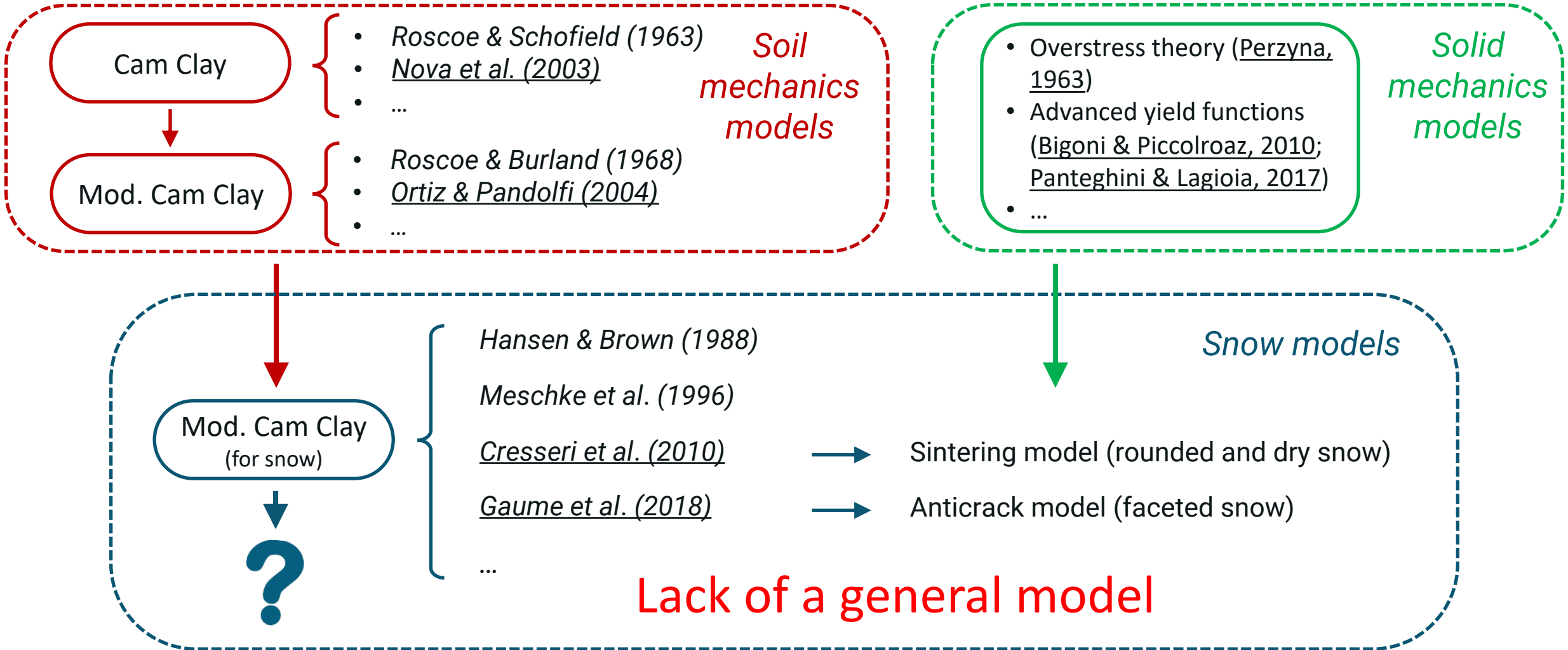


Outlines

1. Introduction
2. The model
3. Numerical implementation
4. Conclusions



1. Introduction: bibliography and state-of-the-art of snow models



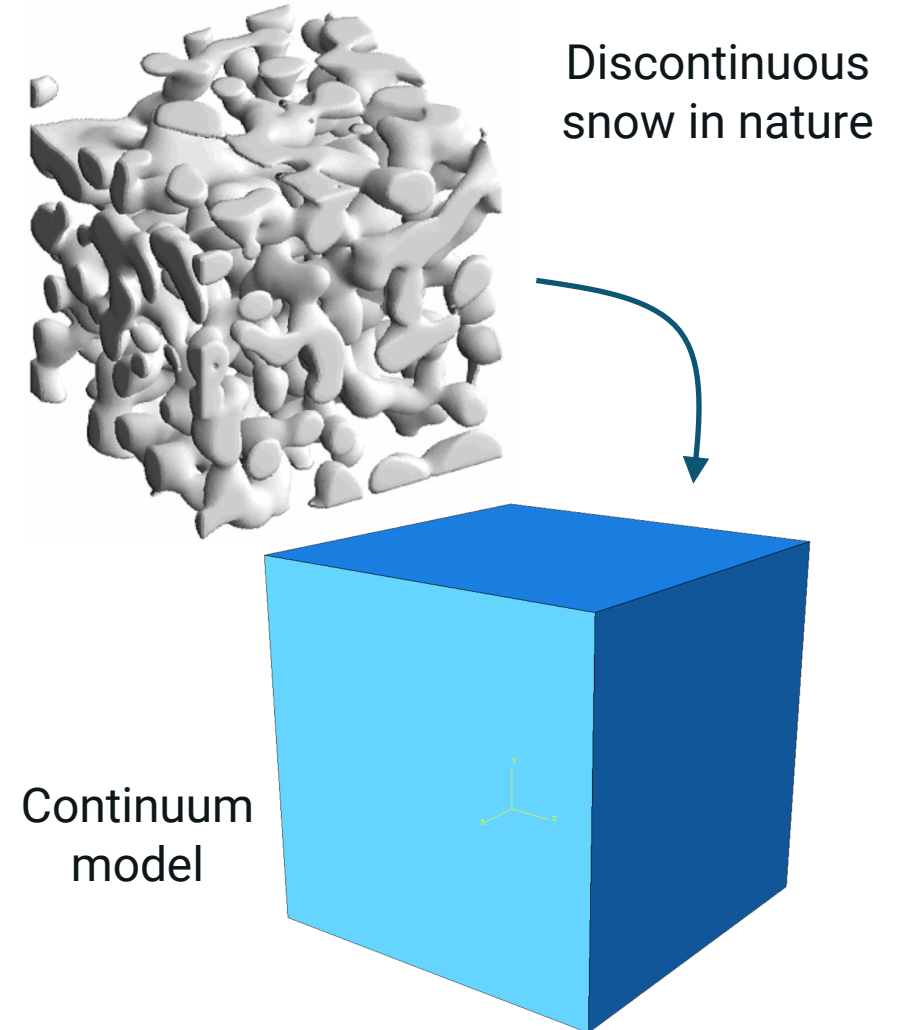
2. The model: general aspects

❄ My initial proposal for the model is based on **three key points**:

1. the general framework of the elastic-visco-plastic model proposed by **Cresseri & Jommi (2005)**
2. the **overstress theory of Perzyna (1963)**, accounting for irrecoverable strains even inside the yield locus
3. A **new formulation for the yield surface**

❄ Initial hypotheses and assumptions: **small strains, continuity, homogeneity, and isotropy**

❄ The **temperature is constant** during the test time (purely mechanical model)



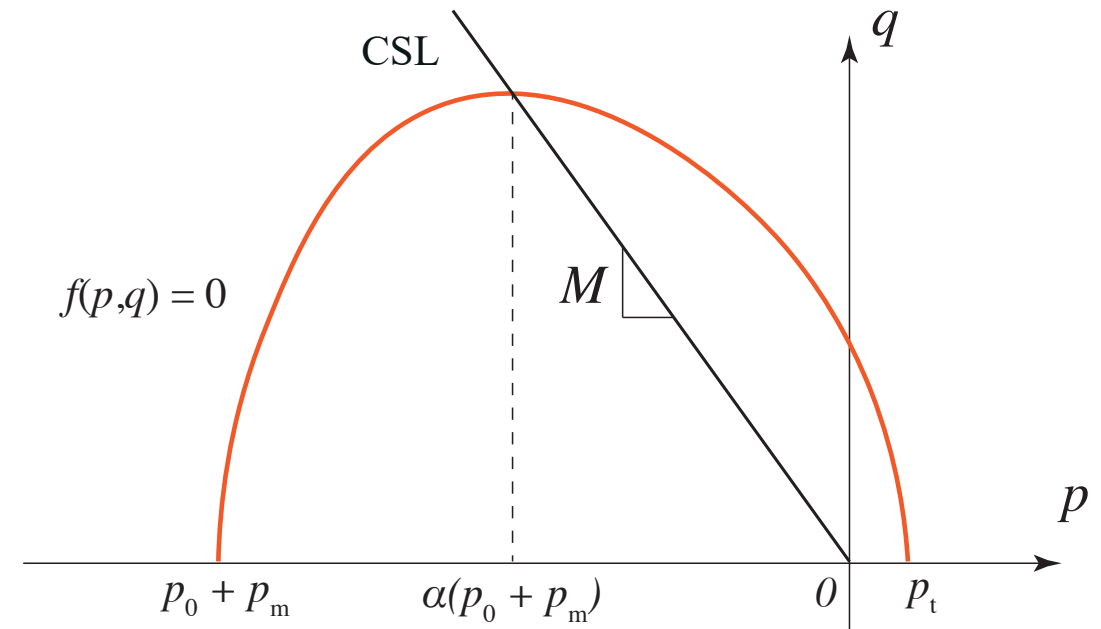
2. The model: yield surface (i)

The model uses an **improved yield surface** that was obtained starting from the Mod. Cam Clay for snow (Cresseri & Jommi, 2005) and the Panteghini & Lagioia (2017) methodology to deform the yield surface

$$f(p, q) = \frac{1}{p_{atm}^2} \left\{ q^2 - 4\alpha^2 M^2 (p_0 + p_m)^3 \frac{\phi_1}{\phi_2^2} \right\}$$

$$\phi_1 = (\alpha - 1)(p - p_t)(p + p_0 + p_m)[p_t + \alpha(p_0 + p_m)]$$

$$\phi_2 = -p(p_0 + p_m - p_t) + 2p(p_0 + p_m)\alpha + (p_0 + p_m)[-(\alpha - 2)p_t + (p_0 + p_m)\alpha]$$



The new surface accounts for the **additional strength in compression** (p_m) and **tension** (p_t) due to sintering

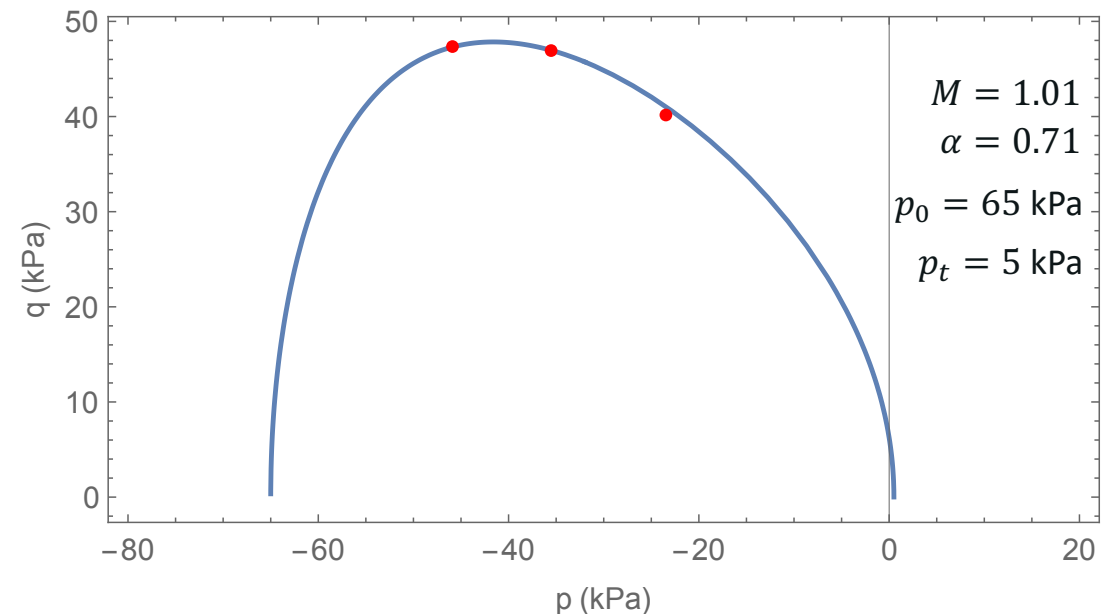
2. The model: yield surface (ii)

The **meridian section of the yield surface** is described by the following function:

$$f(p, q) = \frac{1}{p_{atm}^2} \left\{ q^2 - 4\alpha^2 M^2 (p_0 + p_m)^3 \frac{\phi_1}{\phi_2^2} \right\}$$

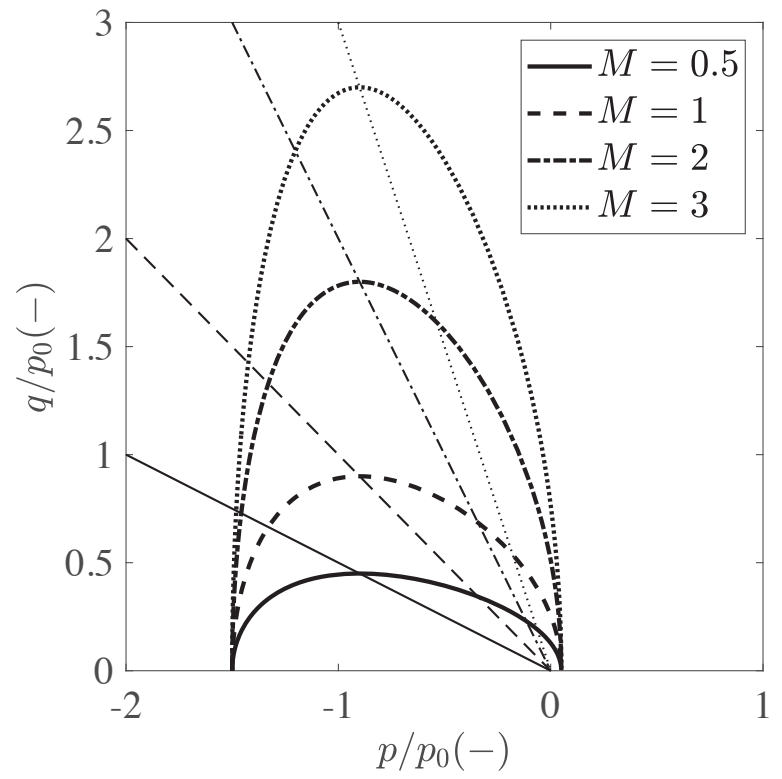
- ❄ The function describes a surface which is **simply convex and smooth** at any point of the p-q space
- ❄ Experimental findings (e.g., Scapozza & Bartelt, 2003) suggest that a asymmetric yield surface is best suited for snow
- ❄ The surface can potentially adapt to various snow conditions (e.g. different grain types, complex stress-paths, etc.)

• = Triaxial data from
Scapozza & Bartelt
(2003)

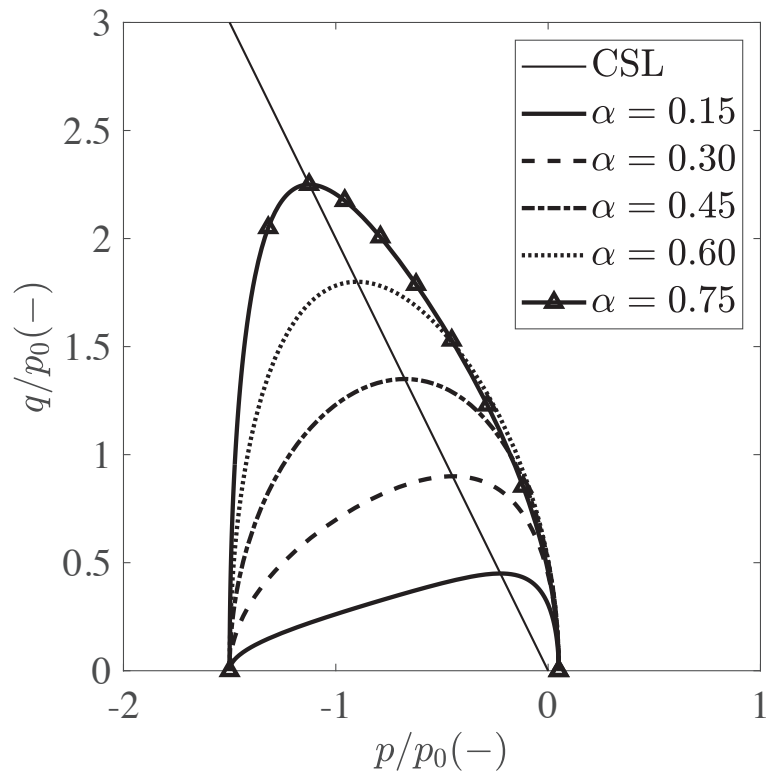


2. The model: yield surface (iii)

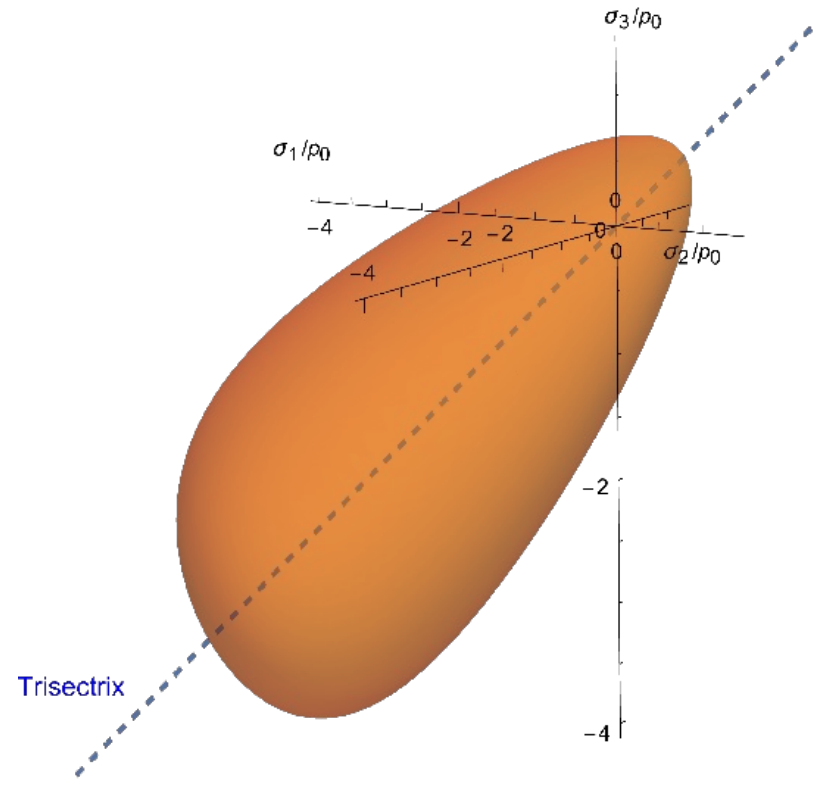
Effect of the shape parameter M on the $f = 0$ curve



Effect of the shape parameter α on the $f = 0$ curve



3D view in the Haigh-Westergaard stress space



2. The model: visco-plastic strain potential

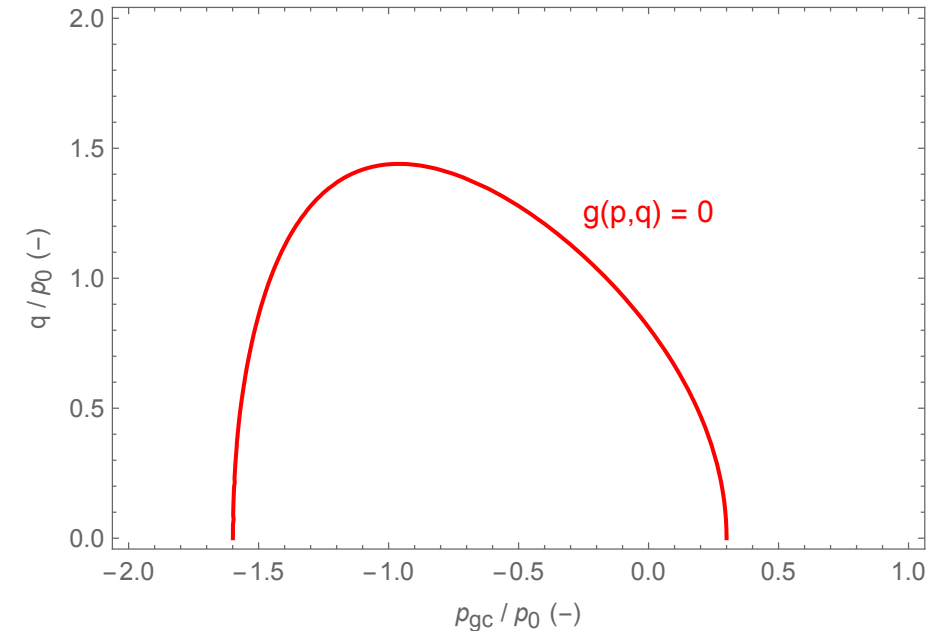
The irreversible strain potential has a mathematical expression quite similar to the yield function

$$g(p, q) = q^2 - 4\alpha^2 M^2 p_{g0}^3 \frac{\phi_{g1}}{\phi_{g2}^2}$$

$$\phi_{g1} = (\alpha - 1)(p - p_{gt})(p + p_{g0})(p_{gt} + \alpha p_{g0})$$

$$\phi_{g2} = -p(p_{g0} - p_{gt}) + 2pp_{g0}\alpha + p_{g0}[-(\alpha - 2)p_{gt} + p_{g0}\alpha]$$

$g(p, q) = 0$ describes a curve passing always through the stress point



Parameters

$$p_0 = 50 \text{ kPa}$$

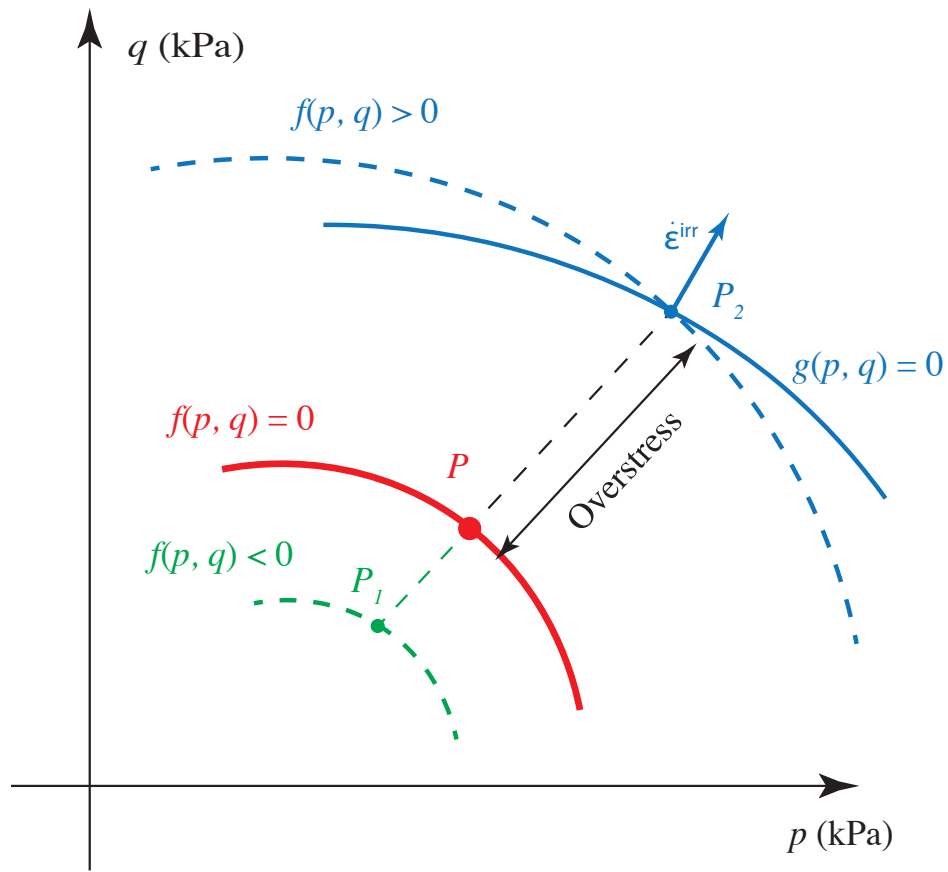
$$p_m = 5 \text{ kPa}$$

$$M = 1.5$$

$$\alpha = 0.6$$

2. The model: flow rule

A **non-associative flow rule of the Perzyna type** is considered to take into account the presence of viscous effects even inside the elastic region (according to Cresseri et al., 2010)



$$\dot{\epsilon}^{irr} = \bar{\gamma} \phi(f) \frac{\partial g}{\partial \sigma} \frac{1}{|\nabla g|}$$

Component	Aspect	Description
Fluidity parameter (always positive)	$\bar{\gamma} = \frac{\psi \sqrt{p^2 + q^2}}{\sqrt{3} p_0}$	Distance of the stress point from the origin
Viscous nucleus (always positive)	$\phi(f) = e^{af}, a > 0$	Component of the deformation velocity, function of the overstress
Normal unit vector	$\frac{\partial g}{\partial \sigma} \frac{1}{ \nabla g }$	direction of the irreversible strains

2. The model: hardening and sintering laws

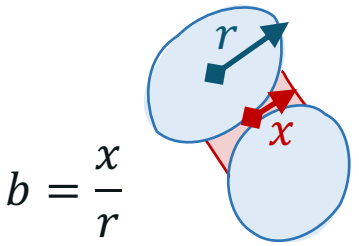
❄️ **Isotropic hardening** rule typical of the Mod. Cam Clay with the addition of the hardening parameter ξ

$$\dot{p}_0 = -\xi \frac{v}{\lambda - \kappa} p_0 \dot{\epsilon}_v^{irr}$$

❄️ The rate of variation of p_m is expressed as:

$$\dot{p}_m = \pi_m b_{max} \dot{S}$$

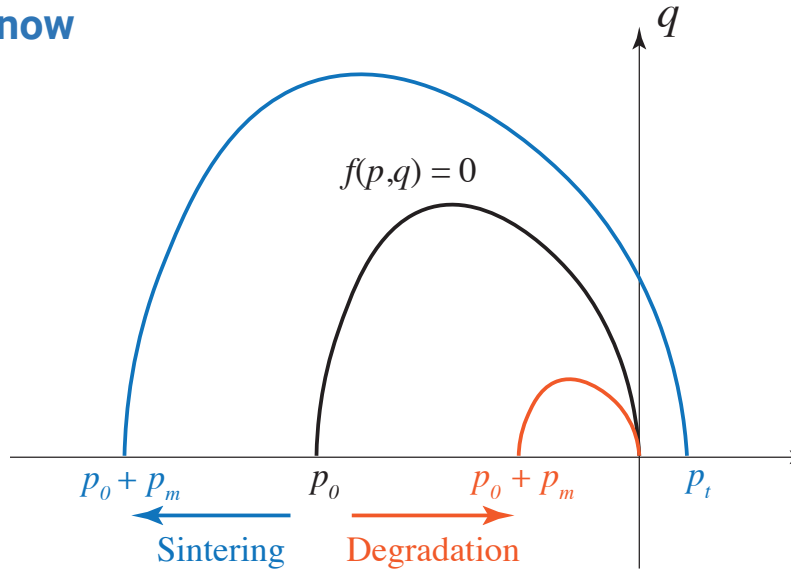
π_m = constitutive parameter
 b_{max} = maximum ratio between the bonding necks and the radius of the particles



❄️ **Sintering law** for snow by Cresseri et al. (2010) describing the current amount of sintering S

$$S = \tilde{S}_0(t_s, r, T) \left[1 - \tanh \left(C \int_0^t \sqrt{(\dot{\epsilon}_v^{irr})^2 + (\dot{\epsilon}_{dev}^{irr})^2} \right) \right]$$

↑
 \tilde{S}_0 = amount of sintering in the unstressed snow
 Degradation term



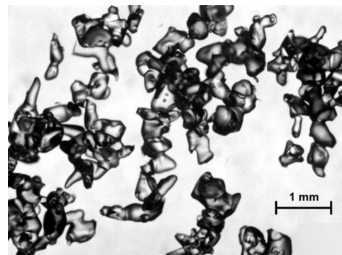
2. The model: parameters

The model is based on **13 parameters** that can be obtained from laboratory tests, observation of the snow grains, literature data, etc.

Parameters	Type	Test for validation
κ, λ, G	Elastic	Triaxial tests, shear tests
M, α, χ, χ_g	Plastic (yield locus)	Shear tests, Compression 1D tests, literature data
ψ, a	Viscous	Compression tests, triaxial tests, relaxation and creep tests, literature data
ξ	Hardening	Literature data, snow grain observation
C, π_m, ω	Sintering	Sintering tests, literature data

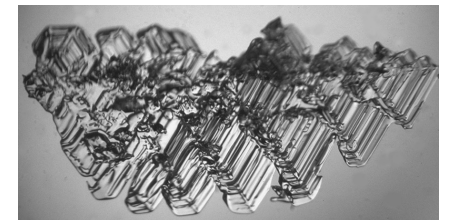
For round snow (hard slab):

$$\begin{aligned}\chi &= \chi_g = 0.05 \div 0.1 \\ \omega &= 0.05 \\ \xi &= 1\end{aligned}$$



For faceted snow (weak layer):

$$\begin{aligned}\chi &= \chi_g = 0 \\ \omega &= 0 \\ \xi &= 0\end{aligned}$$

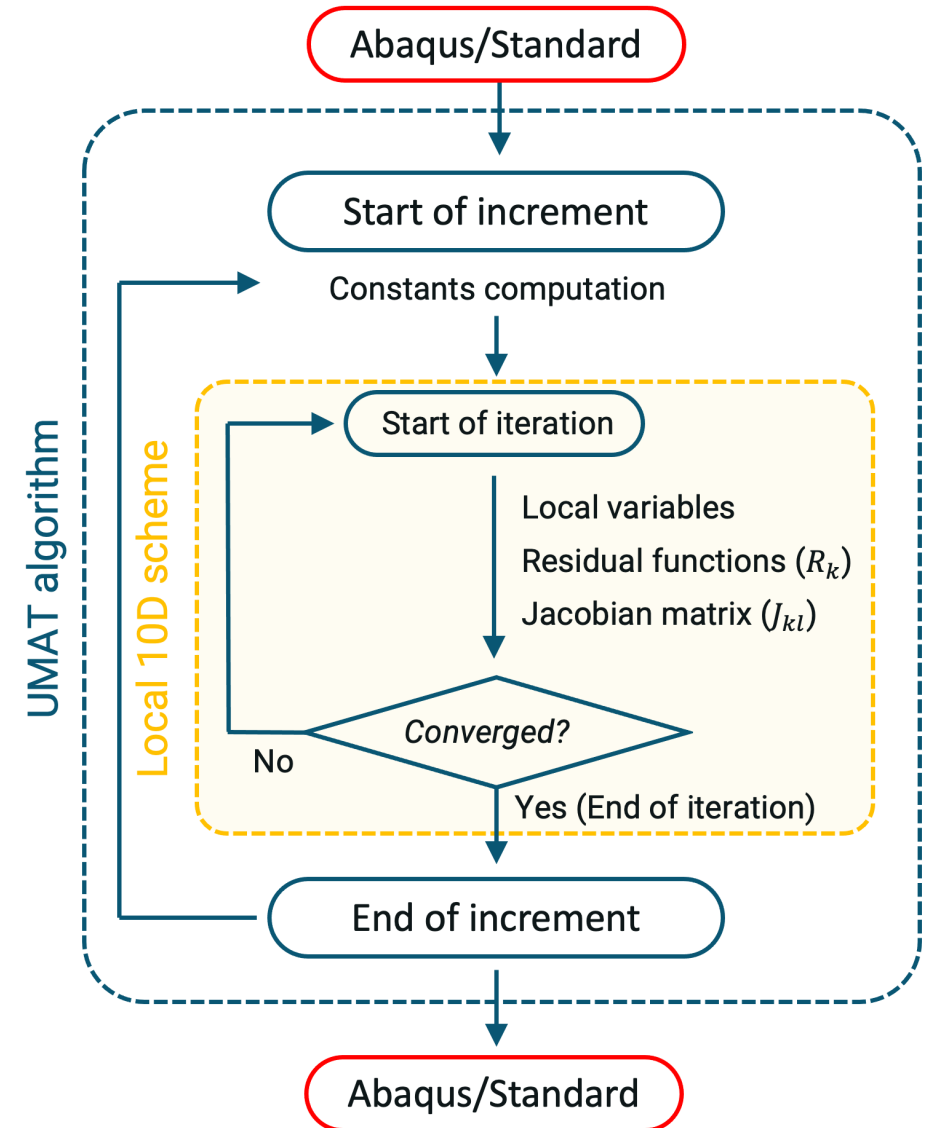
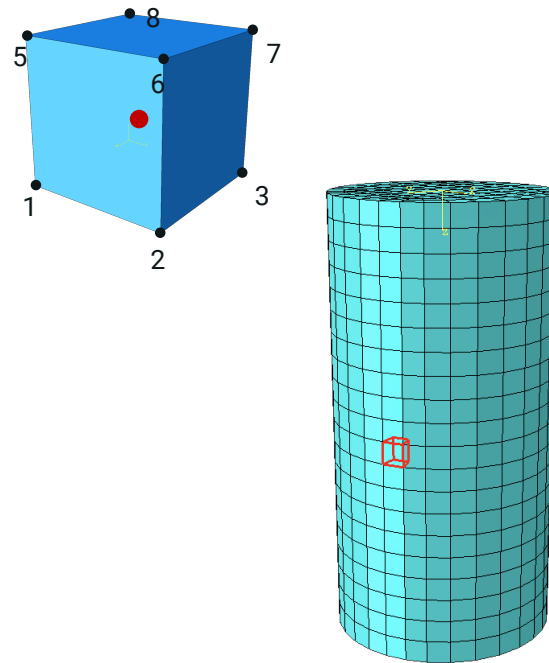


3. Numerical implementation

The model was time-integrated following a **fully implicit backward Euler method scheme**

The **system of 10 non-linear differential constitutive equations** is solved with a local Powell hybrid method (a generalized Newton-Raphson method)

The model has been implemented into the **UMAT format (Fortran 77) for the Abaqus/Standard** Finite Element code



3. Numerical implementation: the 10D discretized system

$$R_{1to6} = \frac{1}{Z_1} \left(\Delta \boldsymbol{\sigma} - \mathbf{D}^e(\boldsymbol{\sigma}_{n+1}) \Delta \boldsymbol{\epsilon} + \mathbf{D}^e(\boldsymbol{\sigma}_{n+1}) \beta_{n+1} \left. \frac{\partial g}{\partial \boldsymbol{\sigma}} \frac{1}{|\nabla g|} \right|_{n+1} \Delta t \right) = 0$$

$$R_7 = \frac{1}{Z_2} \left(g(\boldsymbol{\sigma}_{n+1}, p_{g0}) \right) = 0$$

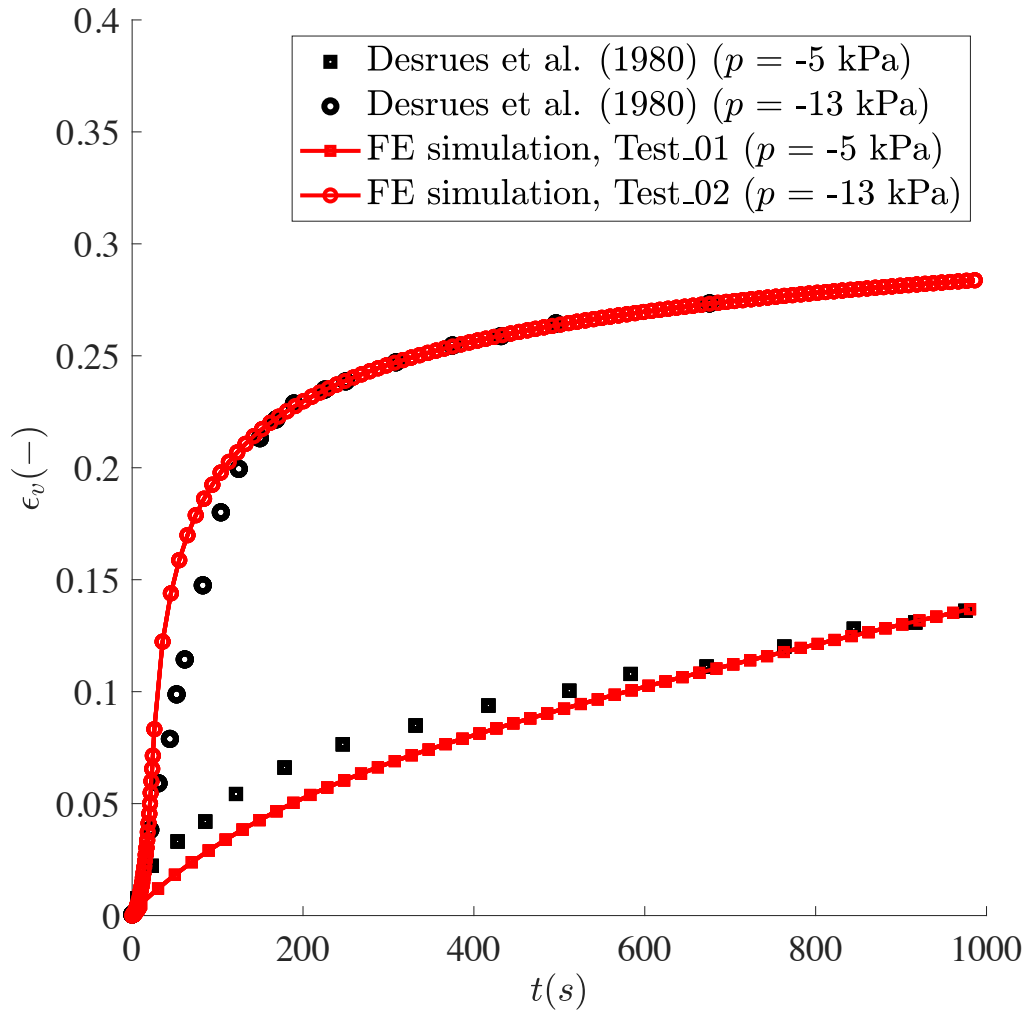
$$R_8 = \frac{1}{Z_1} \left(\Delta p_0 + \xi \frac{v_{n+1}}{\lambda - k} (p_{0n} + \Delta p_0) \Delta \epsilon_v^{\text{irr}} \right) = 0$$

$$R_9 = \Delta p_m - \pi_m b_{max} \Delta S = 0$$

$$R_{10} = S_n + \Delta S - \tanh(\omega t_s) \left\{ 1 - \tanh \left[C \left(\sum_{i=0}^{n-1} \left(\int_{t_i}^{t_i + \Delta t_i} \sqrt{\left(\frac{\epsilon_v^{\text{irr}}}{\Delta t_i} \right)^2 + \left(\frac{\epsilon_{dev}^{\text{irr}}}{\Delta t_i} \right)^2} dt \right) + \int_{t_n}^{t_{n+1}} \sqrt{\left(\frac{\epsilon_v^{\text{irr}}}{\Delta t} \right)^2 + \left(\frac{\epsilon_{dev}^{\text{irr}}}{\Delta t} \right)^2} dt \right) \right] \right\} = 0$$

3. Numerical implementation: some results

Volumetric creep (Desrues et al., 1980)



Initial conditions

Test	p^0 (kPa)	p_0 (kPa)	v_0 (-)	T (°C)	r_0 (mm)
Test_01	0.0	2	4.58	-5	0.2
Test_02	0.0	2	4.58	-5	0.2

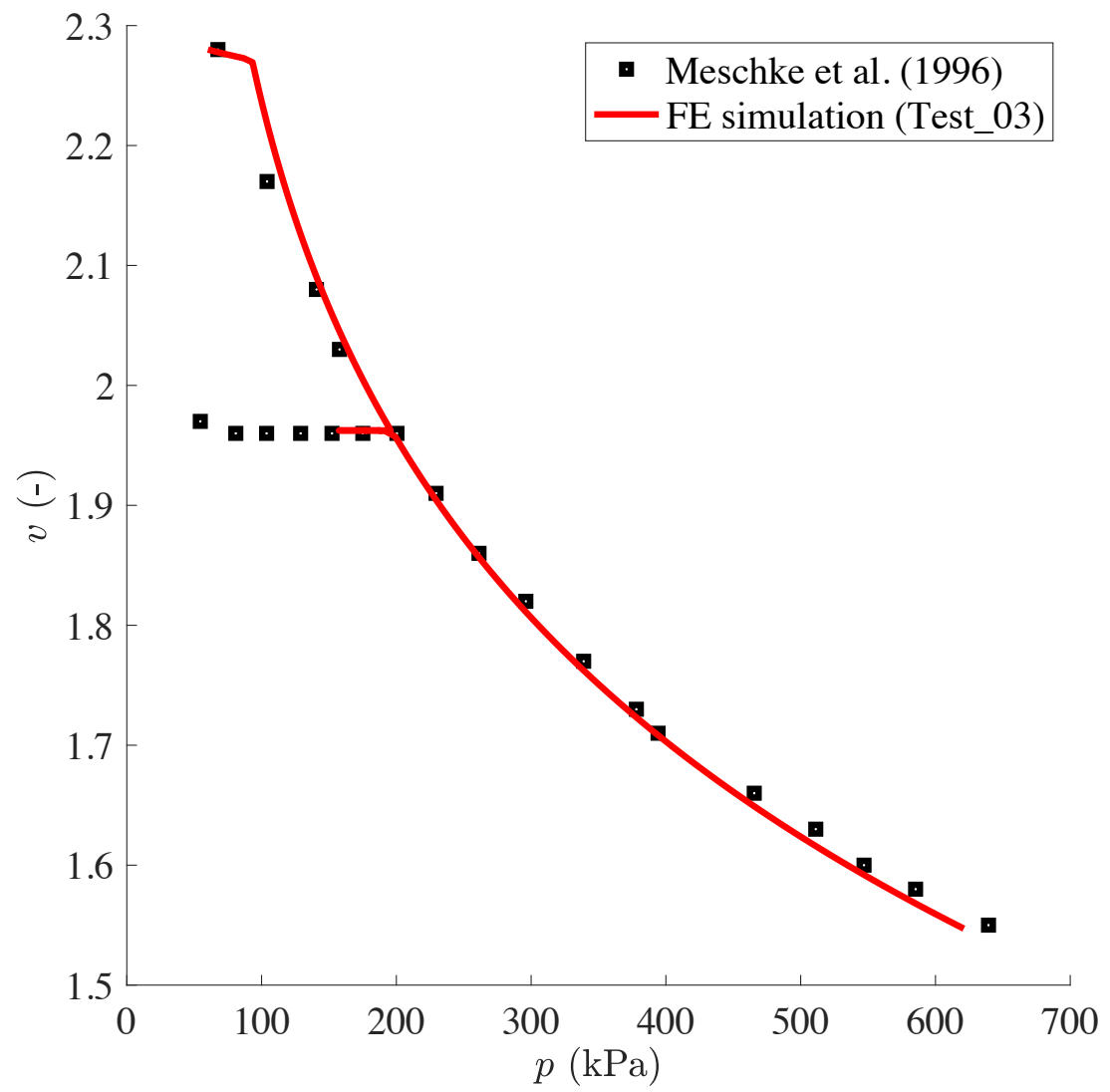
Model parameters

Test	λ (-)	k (-)	G (kPa)	ψ (-)	α (-)	π_m (-)
Test_01 & Test_02	0.35	0.02	2114	1.2e-4	16	40

Test	χ (-)	C (-)	M (-)	α (-)	ξ (-)	ω (-)
Test_01 & Test_02	0.05	0.01	2.88	0.475	1	0.05

3. Numerical implementation: some results

Volumetric compression (Meschke et al., 1996)



Initial conditions

Test	p^0 (kPa)	p_0 (kPa)	v_0 (-)	T (°C)	r_0 (mm)
Test_03	-60.0	77	2.28	-5	0.2

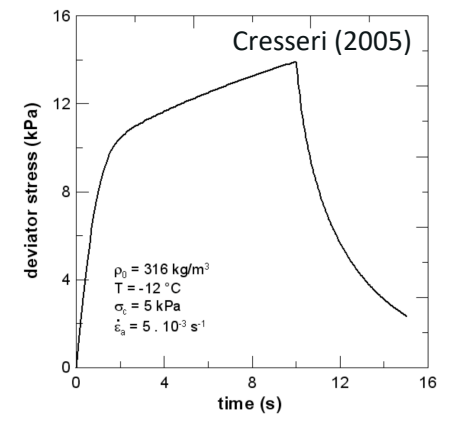
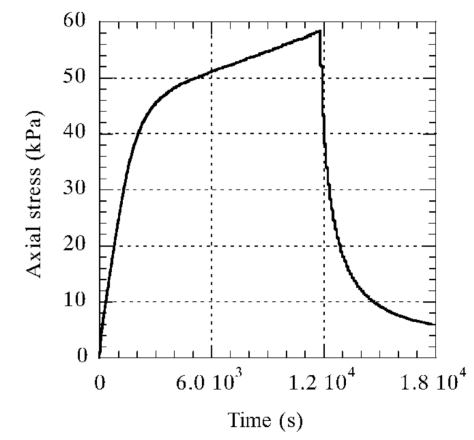
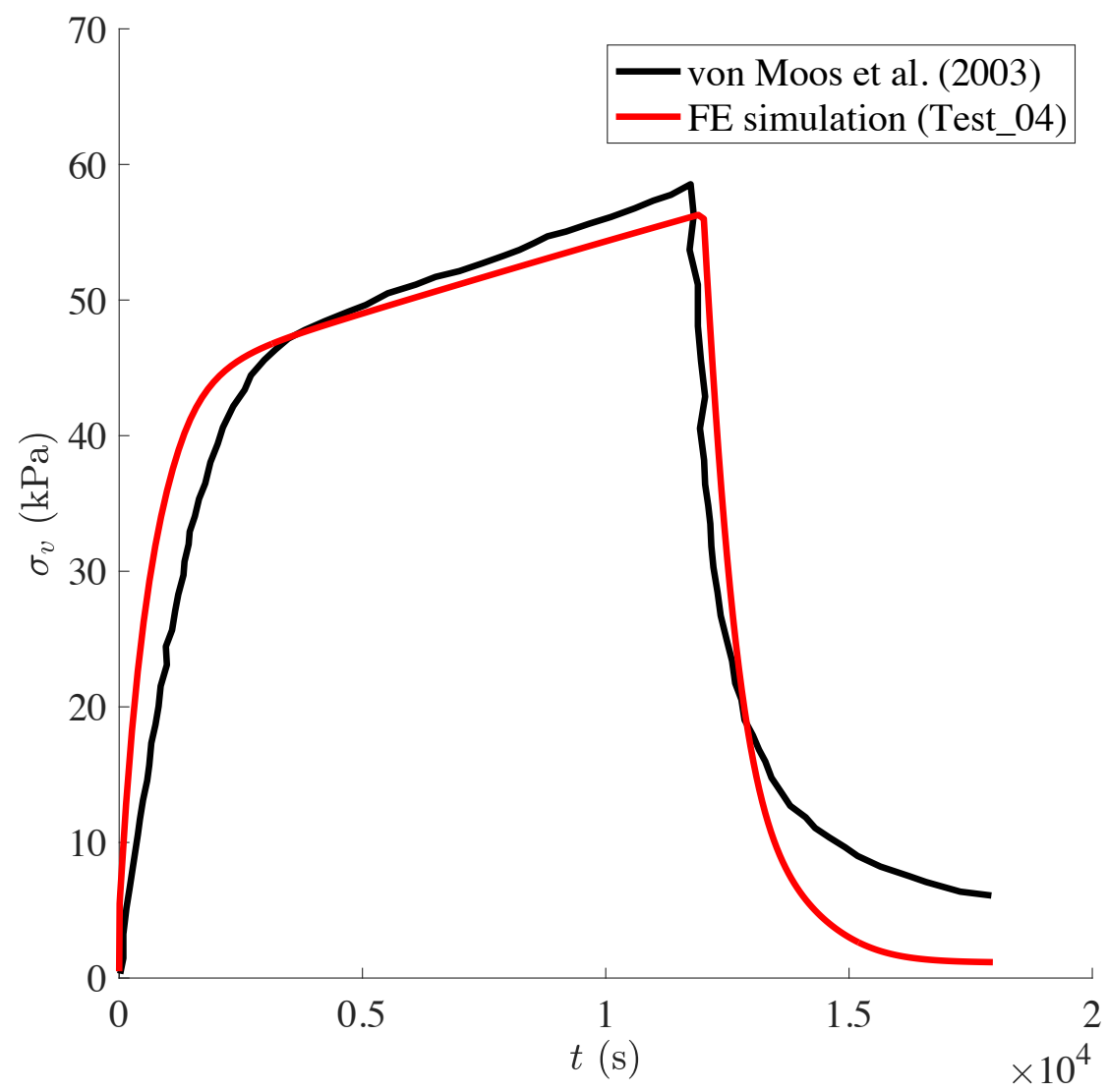
Model parameters

Test	λ (-)	k (-)	G (kPa)	ψ (-)	a (-)	π_m (-)
Test_03	0.35	0.02	12000	2.0e-7	16	40

Test	χ (-)	C (-)	M (-)	α (-)	ξ (-)	ω (-)
Test_03	0.05	0.01	2.88	0.475	1	0.05

3. Numerical implementation: some results

Triaxial compression – long time (von Moos et al., 2003)



Previous FE simulation – only qualitative (Cresseri, 2005)

Initial conditions

Test	p^0 (kPa)	p_0 (kPa)	v_0 (-)	T (°C)	r_0 (mm)
Test_04	0.0	25	2.90	-12	0.118

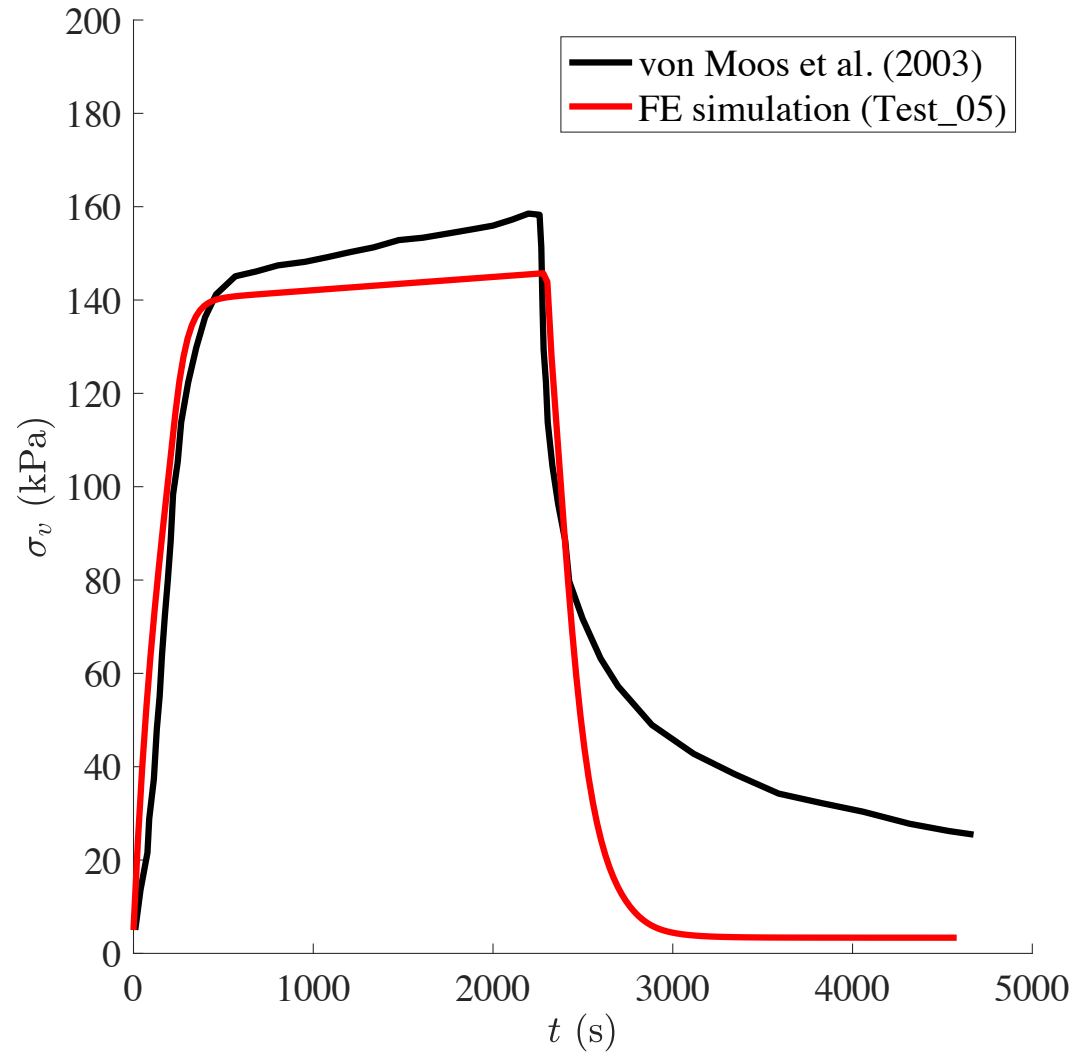
Model parameters

Test	λ (-)	k (-)	G (kPa)	ψ (-)	a (-)	π_m (-)
Test_04	0.35	0.02	8000	4.2e-6	0.35	40

Test	χ (-)	C (-)	M (-)	α (-)	ξ (-)	ω (-)
Test_04	0.05	0.01	2.88	0.475	1	0.05

3. Numerical implementation: some results

Triaxial compression – short time (von Moos et al., 2003)



Initial conditions

Test	p^0 (kPa)	p_0 (kPa)	v_0 (-)	T (°C)	r_0 (mm)
Test_05	-5.0	100	2.44	-12	0.118

Model parameters

Test	λ (-)	k (-)	G (kPa)	ψ (-)	a (-)	π_m (-)
Test_05	0.35	0.02	20000	2.0e-5	0.35	40

Test	χ (-)	C (-)	M (-)	α (-)	ξ (-)	ω (-)
Test_05	0.05	0.01	2.88	0.475	1	0.05

4. Conclusions

- ❄ The model is a **generalization and an improvement of an existing snow model** (Cresseri & Jommi, 2005)
- ❄ The model reproduces satisfactorily different features of the mechanical behavior of snow
- ❄ The model is in **good agreement** (especially from a quantitative point of view) with many lab findings
- ❄ The model can reproduce some tests better than existing snow models
- ❄ **Possible further developments:**
 - i. Consideration of finite strains
 - ii. Definition of specific testing procedures for the identification of model parameters
 - iii. Execution of testing campaigns to extend the available data for parameter estimation



**Politecnico
di Torino**

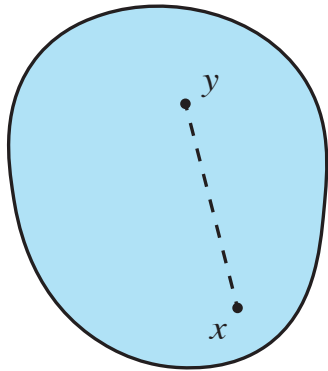
Department
of Structural, Geotechnical
and Building Engineering

Thank you for your kind attention!

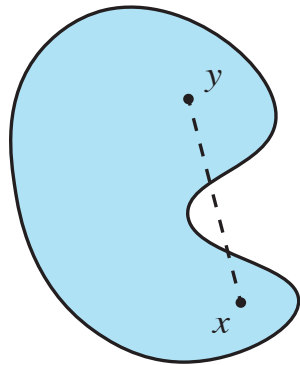
gianmarco.vallero@polito.it

2. The model: convexity (i)

Convexity is a fundamental requirement for the yield surface to guarantee the stability of the model with respect to arbitrary stress and strain paths



Convex set



Non-convex set

A scalar-valued function $f(\boldsymbol{\sigma}, p_c)$ of the stress tensor $\boldsymbol{\sigma} \in D$, where D is a convex subset of \mathbb{R}^6 , and of the hidden variable $p_c \in \mathbb{R}^+$, is **quasi-convex** if all its lower contour sets:

$$L_f(f_0) = \{(\boldsymbol{\sigma} \in D, p_c \in \mathbb{R}^+) | f(\boldsymbol{\sigma}, p_c) \leq f_0\}$$

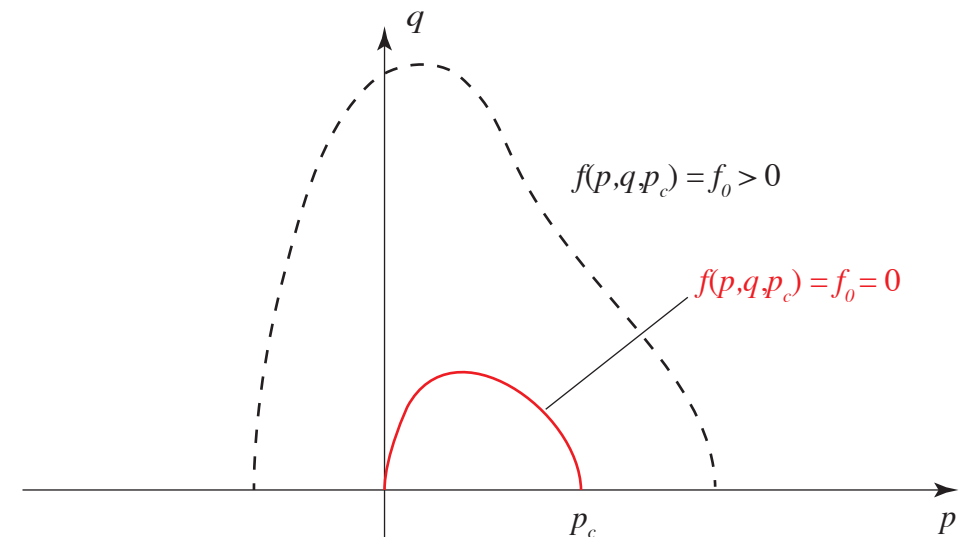
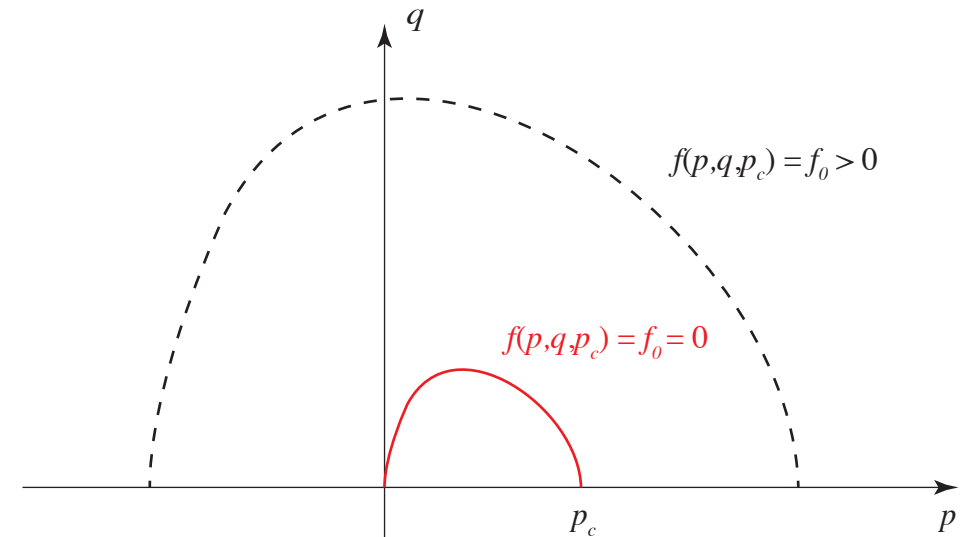
are convex for any $f_0 \in \mathbb{R}$. This relationship needs to be satisfied for any p_c

2. The model: convexity (ii)

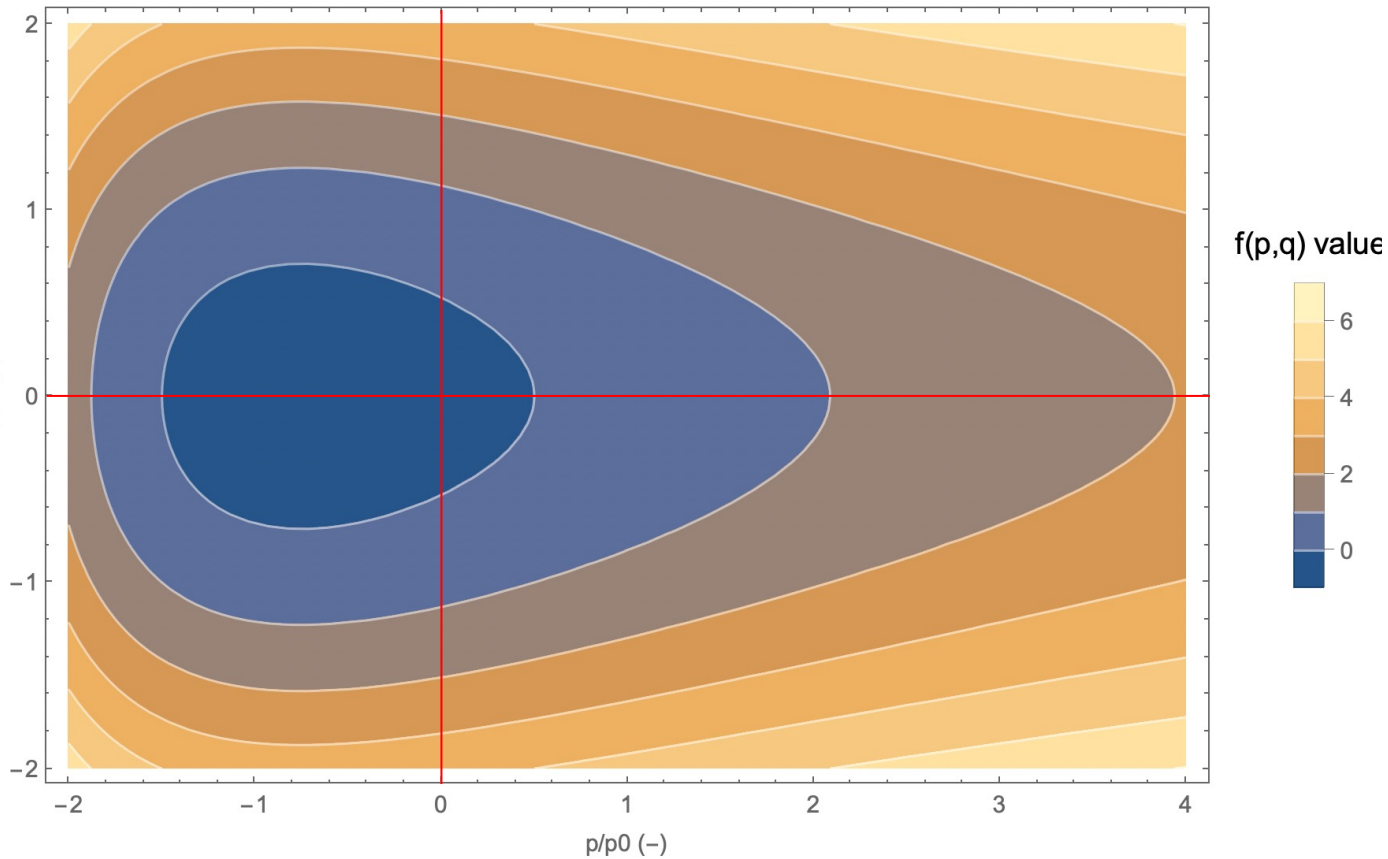
Panteghini & Lagioia (2018) describe two different types of convexity

1. **Simple convexity** indicates that only the zero level set of $f = 0$ is convex (i.e., the yield curve itself) while convexity is lost for all or some values $f = f_0 \neq 0$
2. **Full convexity** indicates that the yield function f is a quasi-convex function, so that any level set $f = f_0$ is convex

The two authors proposed the **convexification technique** to pass from simple to full convexity and to obtain also **linear homothety**



2. The model: convexity (iii)



$$M = 1, \alpha = 0.5, p_m = p_t$$

Here, $f(p, q)$ is a **simply convex function**;
therefore, for “high” values $f > 0$, the convexity
could be lost

In case of Perzyna’s visco-plasticity this could
be a problem even if, for usual snow
applications, f never reaches values higher
than 2

The convexification technique is difficult to
implement

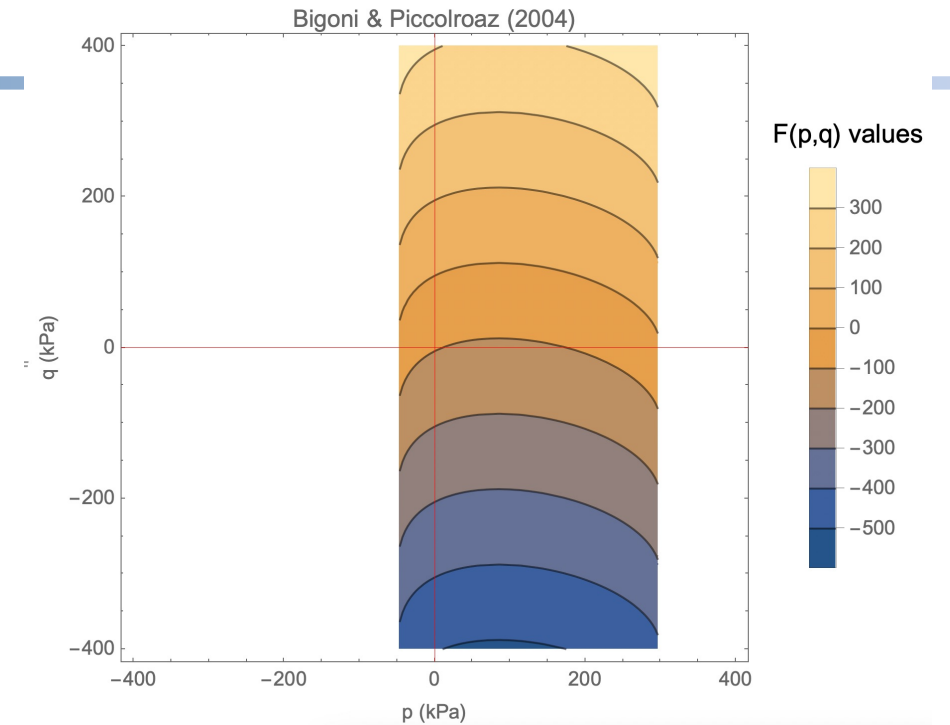
An expression similar to f is used for the **visco-
plastic strain potential** g together with a **non-
associative flow rule**

g is **simply-convex** as well, and its definition
ensures that g is null for any stress state (p, q)
and the direction of the visco-plastic strains is
not affected by the simple convexity

2. The model: convexity (iv)

In literature exist different surface that can change their shape but can have some problems

For instance, the **Bigoni and Piccolroaz (2004)** surface is defined only in a reduced part of the p-q plane



As a possible improvement, a fully convex yield surface could be introduced by means of the convexification process described by Panteghini & Lagioia (2017)

The fully convex surface maintains its convexity when $f > 0$